Available online at www.sciencedirect.com
SCIENCE DIRECT
Nuclear Instruments and Methods in Physics Research A 558 (2006) 497–503
NUCLEAR INSTRUMENTS & METHODS IN PHYSICS RESEARCH Section A
www.elsevier.com/locate/nima

CdZnTe Frisch collar detectors for γ-ray spectroscopy

Alireza Kargar, Andrew M. Jones, Walter J. McNeil, Mark J. Harrison, Douglas S. McGregor*

S.M.A.R.T. Laboratory, Department of Mechanical and Nuclear Engineering, Kansas State University, Manhattan, KS 66506, USA

Received 28 September 2005; accepted 29 November 2005
Available online 21 December 2005

Abstract

Low-energy γ-ray spectra were collected from ^{241}Am, ^{57}Co, ^{133}Ba, ^{198}Au, ^{137}Cs and ^{235}U using a $3.4 \times 3.4 \times 5.7\,mm^3$ CdZnTe detector utilizing an insulated Frisch ring. The CdZnTe detector was fabricated from a single crystal and a copper shim was used as the Frisch collar. Room-temperature energy resolution of 1.45% full-width half-maximum (FWHM) was obtained for ^{137}Cs at 661.7 keV without electronic correction. The detector fabrication process is described and the resulting energy spectra are discussed. The detector fabrication process is described and the resulting energy spectra are discussed. The detector full-energy-peak intrinsic efficiency is reported for different γ-ray energies, specifically from ^{241}Am, ^{57}Co, ^{133}Ba and ^{137}Cs.

PACS: 29.30.Kv; 29.40.−n

Keywords: Gamma ray detector; Gamma ray spectrometer; CdZnTe detector

1. Introduction

CdZnTe has been studied for many years as a material for room-temperature, high-energy resolution γ-ray detectors. Commercial and prototypical detectors are now available for medical imaging, industrial tomography and astrophysics. However, a simple device for accurately identifying radionuclides has not been available until recently with the advent of the semiconductor Frisch collar spectrometer [1–3]. Previous "single carrier" CdZnTe devices either lacked sufficient energy resolution, were complex to operate, or expensive to manufacture.

Energy resolution of planar CdZnTe devices is degraded by poor charge-carrier collection. The problem arises from electron and hole trapping, in which the hole trapping is much more deleterious than the electron trapping. Hole transport properties, such as mobility (μ) and lifetime (τ), within CdZnTe are generally poor compared to many other semiconductor materials. Various methods have been presented to improve the energy resolution of CdZnTe devices, with most methods concentrating on reducing the degrading effects of hole trapping, including variations using the small pixel effect [4], co-planar grids [5], and geometric weighting [6,7].

The virtual Frisch grid effect in solid-state radiation detectors has been studied in various forms to overcome the problem of severe hole trapping [1–3,7–12]. A brief explanation of the Frisch grid effect [13] and its application for a semiconductor device has been previously presented in literature [7,8]. Devices using contacts applied directly to a semiconductor surface have voltage limitations imposed by leakage currents flowing between the virtual grid region and the collecting anodes. Frisch collar planar devices show spectroscopic improvement with minimal leakage current between the grid and anode [1–3,10–12]. The Frisch collar device also shows enhancement in charge collection efficiency without substantially increasing leakage current [3]. Excellent results have been achieved using this technique with the Frisch collar extending the entire length of the detector [12].

It has been shown elsewhere that applying the Frisch collar to a planar detector restructures the weighting potential such that the electrons contribute significantly

*Corresponding author. Tel.: 01 785 532 5284; fax: 01 785 532 7057.
E-mail address: mcgregor@ksu.edu (D.S. McGregor).

0168-9002/$ - see front matter © 2005 Elsevier B.V. All rights reserved.
doi:10.1016/j.nima.2005.11.211

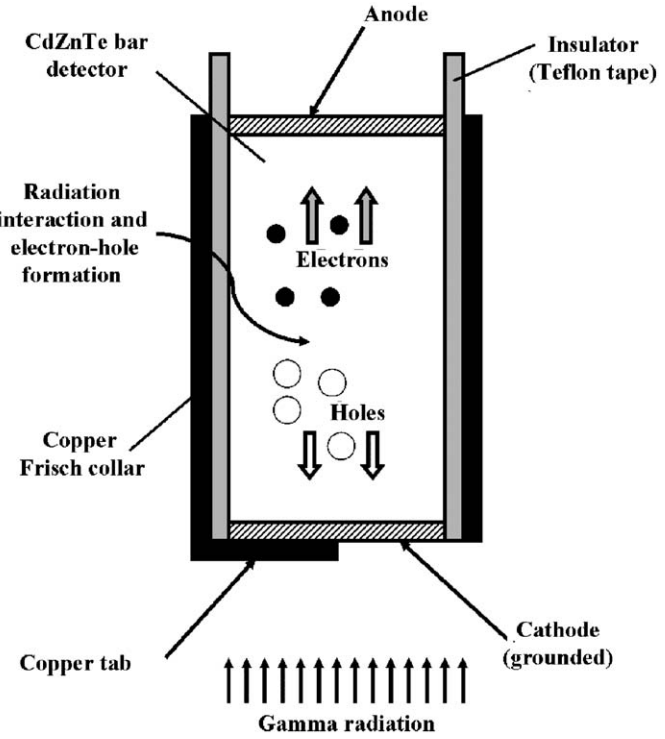

Fig. 1. Diagram of a bar shaped CdZnTe detector with the Frisch collar.

more to the charge induction and detector output pulse [3,10], thereby improving the energy resolution by changing a simple planar detector into a single carrier device. As shown in Fig. 1, for any interaction occurring within the device, charge carriers will be attracted to their respective electrodes. Changes in the weighting potential are largest in the near-anode region; hence the negative charges (electrons) contribute much more to the detector output pulse than the positive charges (holes), as the carriers transit through the detector bulk [3]. Therefore, the induced charge is dominated mainly by the motion of the electrons rather than the motion of the holes. In this way, the effects of hole trapping are nearly eliminated. As a consequence of Frisch collar effect, the observed pulse height is virtually independent of hole motion, and the energy resolution is improved.

2. Experimental procedure

Bulk CdZnTe material acquired from eV products, labeled as "counter grade", was used to fabricate several Frisch ring detectors. The material was initially inspected with an infrared (IR) microscope to locate a region containing relatively few visible defects. A diamond wire saw was then utilized to section volumes with low defect densities from the bulk samples.

The extracted pieces were next shaped, through grinding and lapping, into right parallelepipeds. The sliced material was first ground using an L-shaped stainless-steel jig to form the piece into a rectangular bar shape (Fig. 2a). Silicon carbide (SiC) papers of 2400 and 4000 grit were

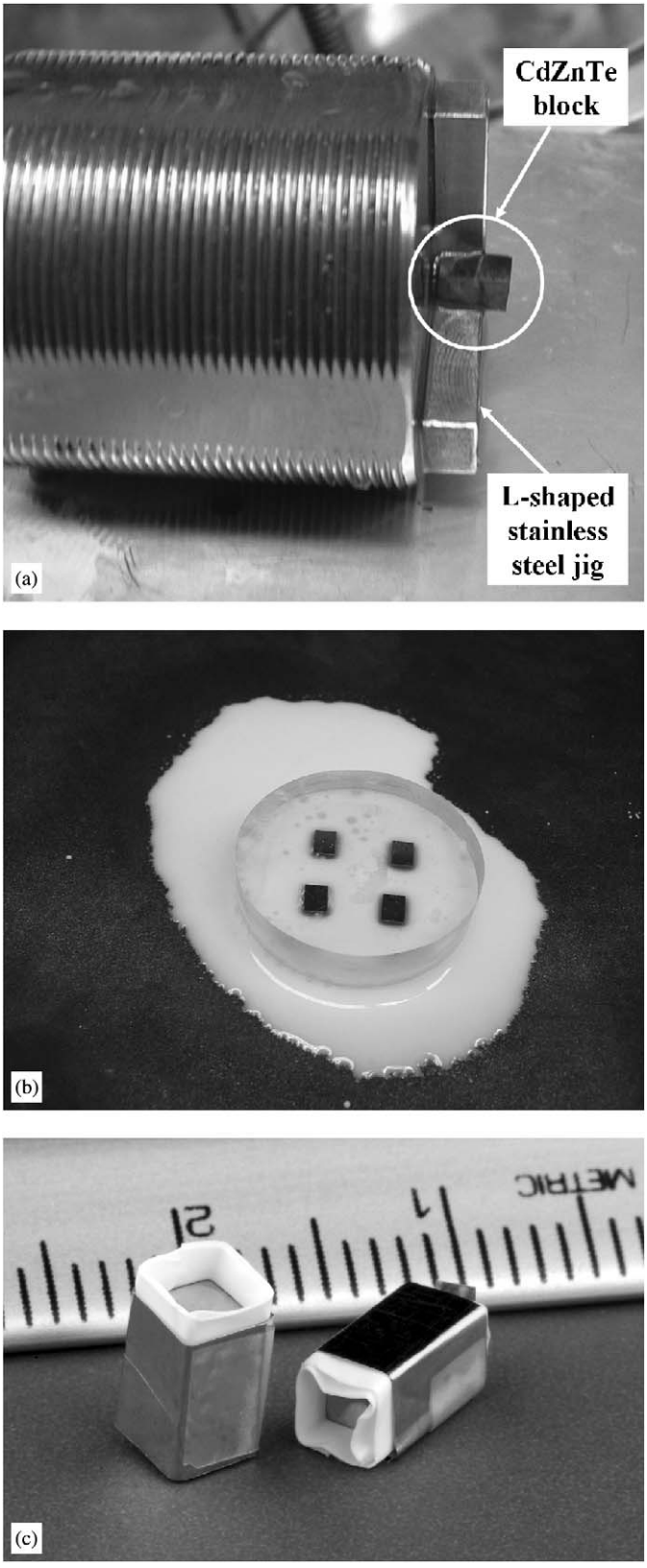

Fig. 2. Steps in the detector fabrication process, showing the (a) grinding/lapping jig, (b) mechanical polishing, and (c) the fabricated 3.4 mm × 3.4 mm × 5.7 mm CdZnTe detectors.

used in the grinding step, in which the pieces were continuously cleaned by running water.

The ends of the bar-shaped crystals were hand lapped with alumina powders suspended in deionized (DI) water, starting with 3 μm powders, and after a progression of diminishing sized powders, ending with 0.05 μm powder on BUEHLER Chemomet polishing cloths (Fig. 2b). The 1 and 0.3 μm alumina powder solutions were used as intermediate polishing steps. At least a total of 500 μm of material was polished away from each of the sides. Mechanical polishing causes surface damage extending into the crystal bulk typically three times the size of the powder being used. Hence, while performing mechanical polishing, it is important to remove all of the surface damage caused in the previous step. Afterward, the samples were rinsed with DI water and isopropyl alcohol before chemical treatment. The rinse was followed by a chemical etching step with a 2% bromine/methanol solution for a 2 min duration. The samples were then rinsed once more with isopropanol.

Gold was deposited on the ends of the crystal to form the ohmic contacts through an electroless deposition technique using gold chloride ($AuCl_3$). The $AuCl_3$ solution was deposited for 8 min on each contact. When gold chloride is applied to the CdZnTe surface, a chemical reaction occurs, in which cadmium is removed from the surface and replaced by gold.

Surface passivation was performed as the final treatment to the devices. An ammonium fluoride (NH_4F)/DI water/hydrogen peroxide (H_2O_2) solution of 2.68 g/17 ml/8 ml was applied to the crystal surfaces for 10 min [14]. Passivation provides an oxide layer that replaces tellurium-rich surfaces left behind by the bromine/methanol etching step. This resistive oxide reduces side-surface leakage current substantially.

Finally, the passivated crystal was wrapped with thin Teflon tape, which acted as an insulating boundary. The Teflon extended beyond the anode about 2 mm in order to avoid discharge between the collar and the anode. A thin copper shim was cut to size and used as the Frisch collar (Fig. 2c). The Frisch collar extended the entire length of the device, and was connected to the device cathode. In this manner, the Frisch collar was held at the cathode potential (or ground).

The fabricated CdZnTe detector, now with a Frisch collar, was positioned in an aluminum test box for spectral collection of various radionuclides (Fig. 3a). The detector within the box was connected to an Ortec Model 142A preamplifier, and the aluminum test box and preamplifier were placed inside a copper Faraday cage to minimize electronic noise. The measurement system consisted of an amplifier, an oscilloscope, a 1024-channel multi-channel analyzer (MCA), a high-voltage supply, a pulse generator and a personal computer, all positioned outside the Faraday cage (Fig. 3b). Gamma sources were always placed in the same position next to the aluminum test box such that the detector cathode faced the source. During the experiment the temperature and the relative humidity were recorded to be near 27 °C and 60%, respectively. Operating parameters were held at a high-voltage bias of 1000 V, amplifier gain of 700 and shaping time of 1 μs. The lower level discriminator (LLD) was varied between 10 and 25 keV equivalent depending on dead time and system noise.

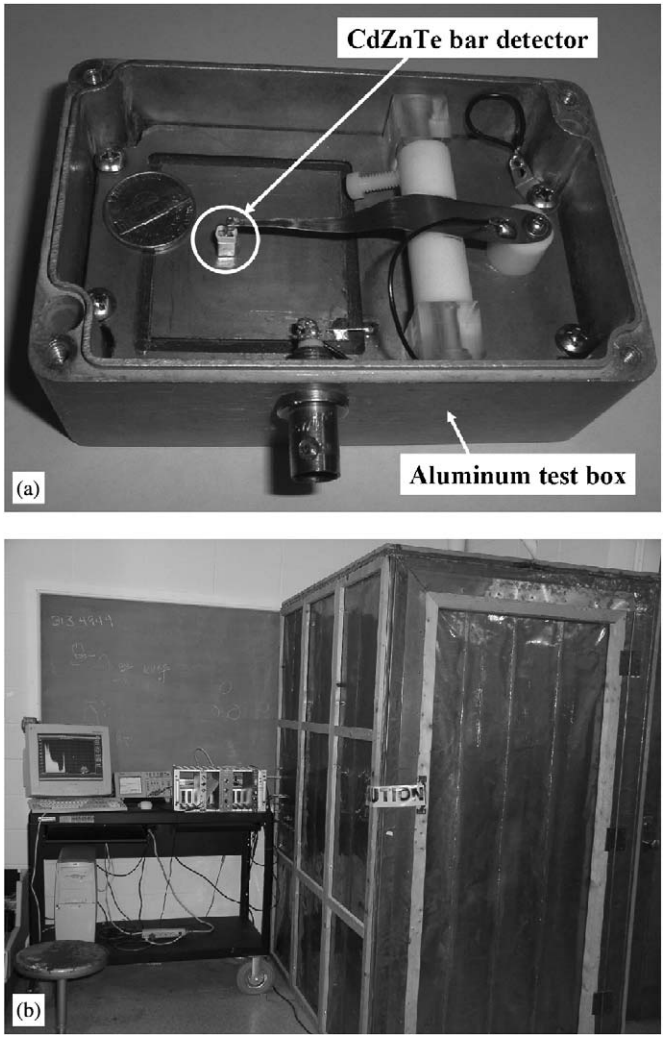

Fig. 3. Experiment apparatus and testing equipment, showing the (a) aluminum test box with an installed CdZnTe Frisch collar device and the (b) Faraday cage and electronics.

3. Results and discussion

3.1. Spectral performance

Pulse height spectra were collected from γ-rays sources of ^{241}Am, ^{57}Co, ^{133}Ba, ^{198}Au, ^{137}Cs and ^{235}U. The ^{241}Am, ^{57}Co, ^{133}Ba and ^{137}Cs samples were standard commercially available calibration sources. The ^{198}Au was prepared through an (n, γ) reaction by irradiating a 13 mg sample of Au foil in the Kansas State University TRIGA Mk II nuclear reactor core for 5 min at a fast neutron flux of $3.5 \times 10^{12}\,cm^{-2}\,s^{-1}$ and thermal flux of $4.3 \times 10^{12}\,cm^{-2}\,s^{-1}$.

The ^{235}U source was in the form of a 93% enriched ^{235}U-nitride solution. The electronic settings were consistent as previously explained for all measurements and energy resolutions reported for γ-ray photopeaks are without any electronic corrections.

An energy resolution of 9.10% (5.41 keV) FWHM for the 59.5 keV spectral line of ^{241}Am was obtained. The evaluated energy resolution is shown in Fig. 4 and does not take into consideration any contributions from electronic noise. The low-noise floor and the high resolution of the device allows for the discernment of Cd and Te X-ray escape peaks, as labeled near 35 keV.

A ^{57}Co spectrum is shown in Fig. 5. The energy resolution at the 122 keV photopeak is 4.91% (5.99 keV) FWHM and the 136 keV photopeak is clearly observed as a small peak on the right side of the 122 keV photopeak. The Cd and Te X-ray escape peaks are also visible. An electronic pulser peak is shown in the spectrum for electronic noise comparisons, and is located near 191 keV on the energy scale.

Figs. 6–8 display the energy spectra for ^{133}Ba, ^{198}Au, and ^{137}Cs, respectively. An energy resolution of 7.55% (6.04 keV) FWHM was achieved for the 80 keV photopeak of ^{133}Ba as shown in Fig. 6a. The 356 keV photopeak of ^{133}Ba exhibited an energy resolution of 2.33% (8.29 keV) FWHM (see Fig. 6b). The full energy peaks corresponding to the 276, 302 and 382 keV emission energies of ^{133}Ba are also clearly present in Fig. 6b. The 20 keV low noise cut off makes the device capable of detecting the cesium (Cs) X-rays seen in Fig. 6a. The ^{198}Au spectrum is illustrated in Fig. 7, with an observed full energy peak resolution for the 412 keV emission of 2.26% (9.31 keV) FWHM. Again, the Cd and Te X-ray escapes are observable. The 662 keV photopeak of ^{137}Cs is observed with 1.45% (9.6 keV) FWHM energy resolution. The Compton continuum and backscatter peak are clearly seen in Fig. 8. Due to low noise, barium X-rays are also easily identified.

Fig. 9 shows the energy spectrum of ^{235}U obtained from a low-activity 93% enriched ^{235}U-nitride solution. The

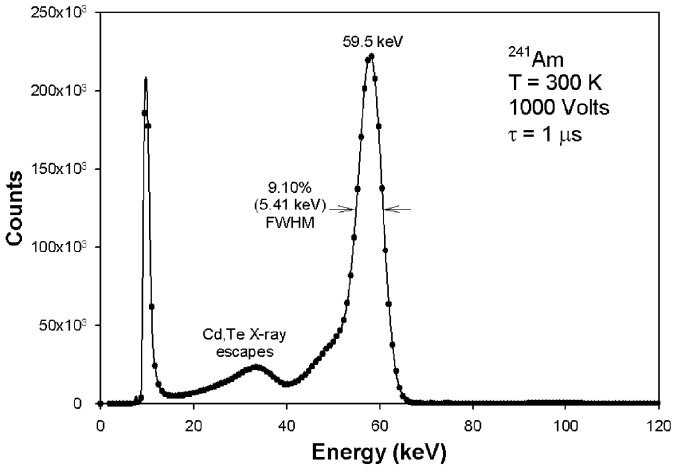

Fig. 4. Room temperature spectrum of a ^{241}Am source from the 3.4 mm × 3.4 mm × 5.7 mm CdZnTe semiconductor Frisch collar detector.

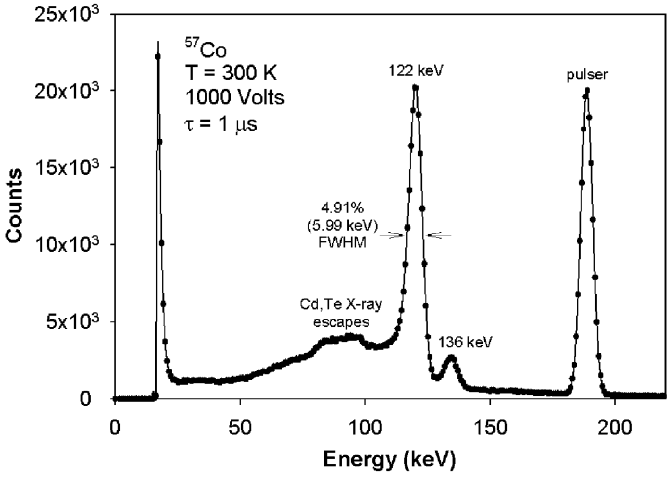

Fig. 5. Room temperature spectrum of a ^{57}Co source from the 3.4 mm × 3.4 mm × 5.7 mm CdZnTe semiconductor Frisch collar detector.

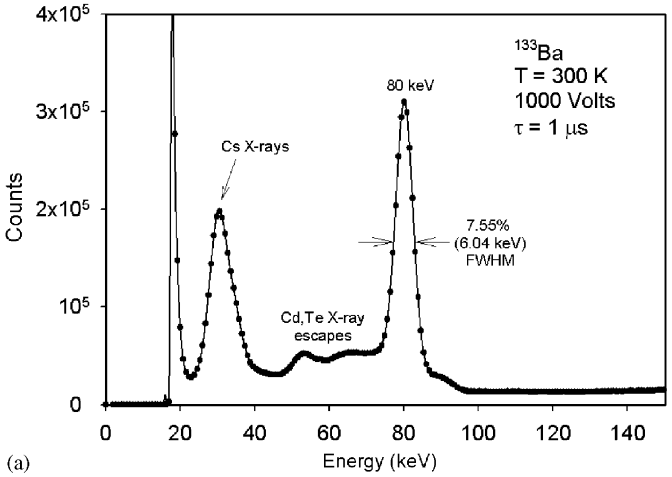

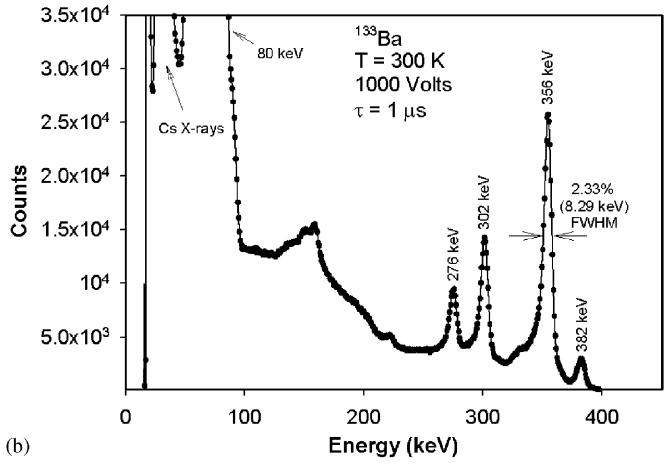

Fig. 6. Room temperature spectra of a ^{133}Ba source from the 3.4 mm × 3.4 mm × 5.7 mm CdZnTe semiconductor Frisch collar detector for (a) low energies and (b) higher energies.

distance between the detector and the source was approximately 5 cm and the exposure time was 20 h. All expected energy emissions, along with their branching

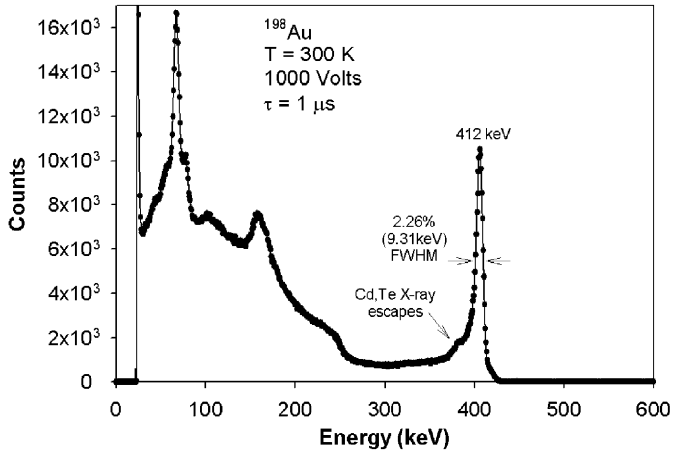

Fig. 7. Room temperature spectrum of a ^{198}Au source from the 3.4 mm × 3.4 mm × 5.7 mm CdZnTe semiconductor Frisch collar detector.

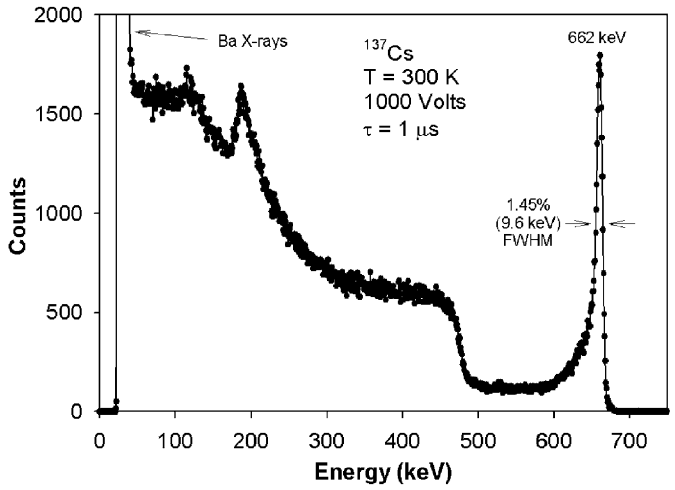

Fig. 8. Room temperature spectrum of a ^{137}Cs source from the 3.4 mm × 3.4 mm × 5.7 mm CdZnTe semiconductor Frisch collar detector.

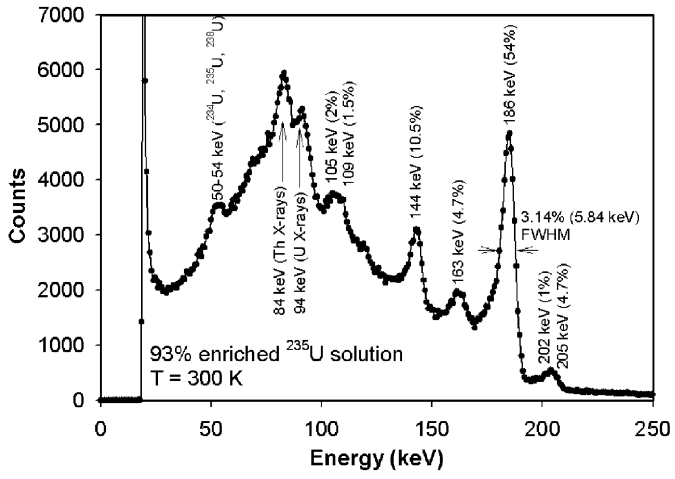

Fig. 9. Room temperature spectrum of a ^{235}U source from the 3.4 mm × 3.4 mm × 5.7 mm CdZnTe semiconductor Frisch collar detector.

ratios, are illustrated in Fig. 9. The clearly distinguishable spectral lines of ^{235}U (Fig. 9) confirms that the insulated Frisch collar design incorporating bar-shaped CdZnTe material is fully capable of radioactive material identification.

As mentioned previously, the energy resolution presented for the photopeaks is without any electronic correction. The pulser energy resolution (2.90% FWHM at 191 keV) in Fig. 5 represents electronic noise contributions to the detector resolution. The standard deviation, σ (FWHM $= 2.35\sigma$), corresponding to the resolution of a full energy peak, is the quadrature sum of the standard deviation values for the detector and the value due to the noise,

$$\sigma^2 = \sigma^2_{\text{detector}} + \sigma^2_{\text{noise}} \quad (1)$$

in which the standard deviation, σ, has the units of energy. It can be seen that in the present case electronic noise

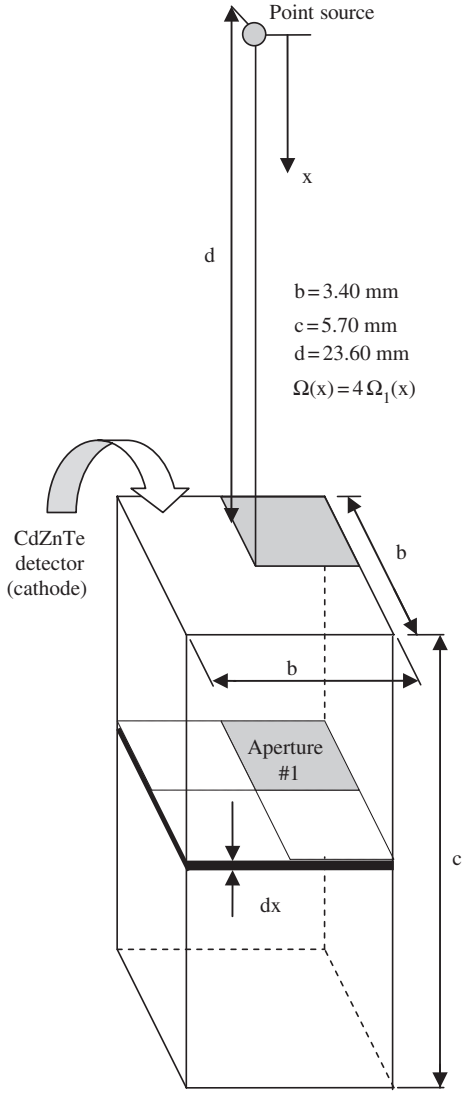

Fig. 10. The solid angle between a point isotropic source and a CdZnTe bar detector with a rectangular aperture with the source aligned along the center of the detector.

contributes significantly to the resolution degradation; hence, by reducing electronic noise in the present system, energy resolution can be significantly improved.

3.2. Intrinsic efficiency calculation of the detector

The intrinsic efficiency of a detector is defined as the ratio of the number of pulses produced by the detector to the number of gamma ray quanta incident on the detector. Clearly, in γ-ray detection, a high-quality detector must be capable of absorbing a large fraction of incident gamma rays. Since high Z number materials result in higher attenuation coefficients for γ-ray absorption, good γ-ray absorption is accomplished by using materials of suitably high Z number [15].

Intrinsic efficiency, $\varepsilon(E)$, can be defined as [15]

$$\varepsilon(E) = \frac{r(E)}{\Omega_{\text{ave}}\,\text{BR}(A_0 e^{-\lambda t})}, \tag{2}$$

where $A_0e^{-\lambda t}$ is the activity of the source during the measurement, $r(E)$ the total number of counts due to full energy absorption per unit time (this value was evaluated for standard sources of ^{241}Am, ^{133}Ba, ^{57}Co and ^{137}Cs by taking the net area under the full energy peak of the corresponding spectrum over the counting time), BR the branching ratio for the specific energy E of gamma ray emitted by the source, $\varepsilon(E)$ the intrinsic efficiency of the CdZnTe detector at energy E of the emitted γ-ray, Ω_{ave} the average fractional solid angle for the entire volume of CdZnTe bar detector exposed to the point source.

With the aim of evaluating the average solid angle, Ω_{ave}, the definition for the average of a function over an interval is applied

$$\Omega_{\text{ave}} = \frac{1}{c}\int_{d}^{d+c} \Omega(x)\,\mathrm{d}x. \tag{3}$$

In this equation, $\Omega(x)$ is the solid angle for the cross-sectional area of CdZnTe detector exposed to the point source at distance x on Fig. 10. The detector dimensions of the bar are illustrated in Fig. 10 as b and c, while the point isotropic source is located at distance d away from the center of the detector.

From literature [15],

$$\Omega(x) = 4\Omega_1(x), \tag{4}$$

where $\Omega_1(x)$ is solid angle of the rectangular 'Aperture #1' shown on Fig. 10, while the point isotropic source is located at distance x away from Aperture #1 and aligned with its corner located in the center of the device. Then, $\Omega_1(x)$ can be evaluated from

$$\Omega_1(x) = \frac{1}{4\pi}\operatorname{atan}\left[\frac{(b/2)^2}{x\sqrt{2(b/2)^2 + x^2}}\right]. \tag{5}$$

Hence, by substituting Eqs. (4) and (5) into Eq. (3), Ω_{ave}

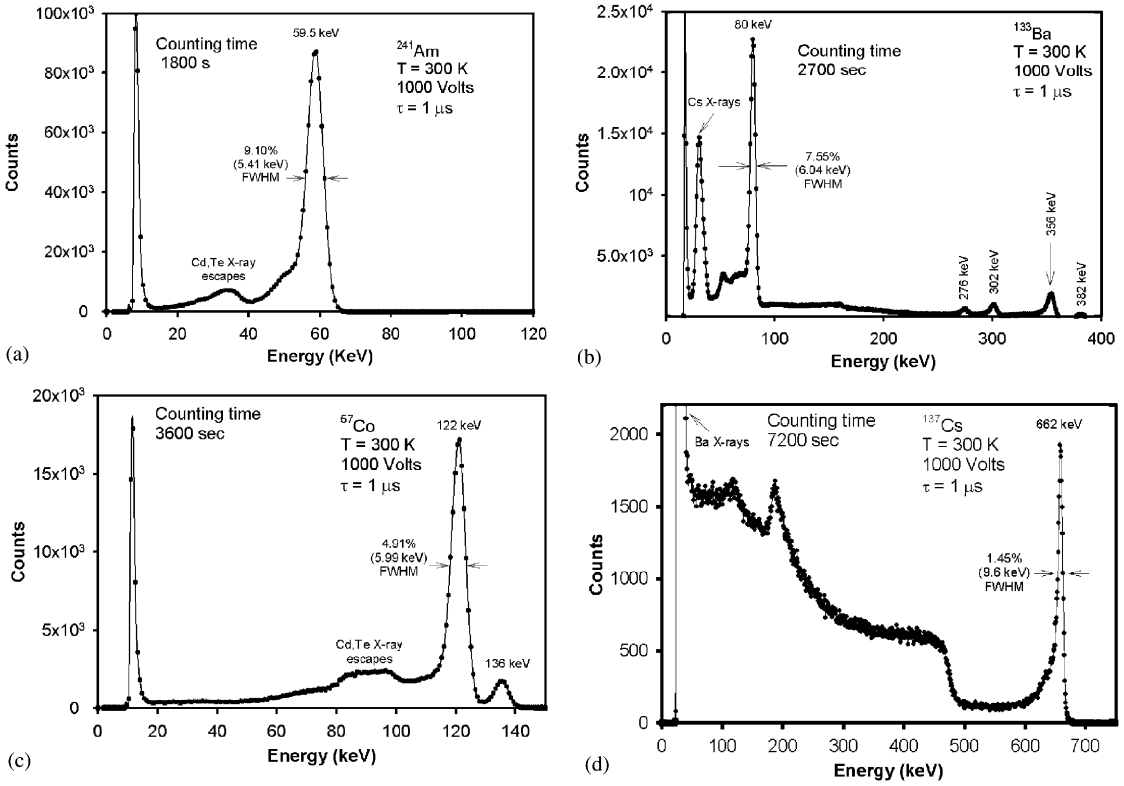

Fig. 11. Room temperature spectra from standard radiation sources taken with the 3.4 mm × 3.4 mm × 5.7 mm CdZnTe semiconductor Frisch collar detector, showing (a) ^{241}Am (1800 s counting time), (b) ^{133}Ba (2700 s counting time), (c) ^{57}Co (3600 s counting time), and (d) ^{137}Cs (7200 s counting time).

Table 1
Summary of the values to determine the intrinsic full energy peak efficiency

Gamma source	^{241}Am	^{133}Ba	^{57}Co	^{133}Ba	^{137}Cs
Energy (keV)	59.5	80	122	356	662
Total counts (G)	710165	192231	159753	23803	41137
Back ground (B)	137726	43180	29738	6300	9590
Counting time (s)	1800	27000	3600	27000	7200
Activity, A_0 (kBq)	1000.00	37.00	380.36	37.00	358.16
Assay date	9/02	11/98	10/03	11/98	10/03
Efficiency $\varepsilon(E)$	0.6743	0.5196	0.5153	0.0335	0.0114
Std. error $\pm\Delta\varepsilon(E)$	0.0011	0.0017	0.0017	0.0003	0.0001

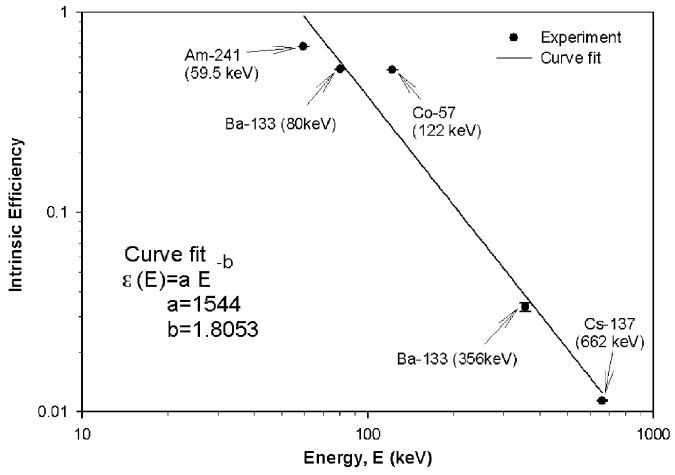

Fig. 12. The measured CdZnTe Frisch collar detector full energy peak intrinsic efficiency at different γ-ray energies.

can be numerically calculated, which was determined to be 0.00132 for the geometry illustrated in Fig. 10.

In order to be consistent with the detector-source geometry, the spectral collection of standard radionuclides was repeated. These energy spectra for ^{241}Am, ^{133}Ba, ^{57}Co and ^{137}Cs are displayed in Figs. 11a–d. The intrinsic efficiency of the detector is summarized in Table 1. The uncertainty calculations are also performed and shown in Table 1, assuming that the uncertainty is due to counting statistics alone. The results for intrinsic efficiencies are plotted for different gamma ray energies in Fig. 12. As expected, the intrinsic efficiency decreases with energy.

4. Conclusion

A $3.4 \times 3.4 \times 5.7\,\text{mm}^3$ bar-shaped Frisch collar CdZnTe detector was successfully fabricated and tested for gamma ray spectroscopy. An energy resolution of 1.45% (9.6 keV) FWHM at 662 keV was obtained without electronic correction. Clearly, these simple CdZnTe semiconductor detectors have excellent energy resolution at room temperature, which is useful in a great number of applications such as remote field operations. The simplistic configuration of the Frisch collar device, which converts a simple planar device into a high-energy-resolution γ-ray spectrometer, is less expensive to manufacture than other "single carrier" designs. Further, due to CdZnTe material growth issues and problems, it is far easier to extract small samples similar to those used in the present work from a commercial ingot than large pieces typically used in other "single carrier' configurations, hence further reducing overall cost. Finally, the devices can be arranged in an array to produce γ-ray imaging devices for medical and isotope identification purposes.

Acknowledgements

Funding was provided by the U.S. Department of Energy through NEER Grant DE-FG07-03ID14498.

References

[1] D.S. McGregor, R.A. Rojeski, US Patent no. 6,175,120, January 16, 2001.
[2] D.S. McGregor, US Patent no. 6,781,132, August 24, 2004.
[3] W.J. McNeil, D.S. McGregor, A.E. Bolotnikov, G.W. Wright, R.B. James, Appl. Phys. Lett. 84 (2004) 1988.
[4] H.H. Barrett, J.D. Eskin, H.B. Barber, Phys. Rev. Lett. 75 (1995) 156.
[5] P.N. Luke, IEEE Trans. Nucl. Sci. NS-42 (1995) 207.
[6] H.I. Malm, C. Canali, J.W. Mayer, M.A. Nicolet, K.R. Zanio, W. Akutagawa, Appl. Phys. Lett. 26 (1975) 344.
[7] D.S. McGregor, R.A. Rojeski, IEEE Trans. Nucl. Sci. NS-46 (3) (1999) 250.
[8] D.S. McGregor, Z. He, H.A. Seifert, R.A. Rojeski, D.K. Wehe, IEEE Trans. Nucl. Sci. NS-45 (1998) 443.
[9] K. Parnham, J.B. Glick, Cs. Szeles, K.G. Lynn, J. Cryst. Growth 214/215 (2000) 1152.
[10] G. Montemont, M. Arques, L. Verger, J. Rustique, IEEE Trans. Nucl. Sci. NS-48 (3) (2001) 278.
[11] L. Cirignano, H. Kim, K. Shah, M. Klugerman, P. Wong, M. Squillante, L. Li, Proc. SPIE 5198 (2004) 1.
[12] A.E. Bolotnikov, G.S. Camarda, G.A. Carini, G.W. Wright, L. Li, A. Burger, M. Groza, R.B. James, Phys. Stat. Sol. (C) 2 (5) (2005) 1495.
[13] O. Frisch, Br. At. Energy Rep. BR-49 (1944).
[14] G.W. Wright, G. Camarda, E. Kakuno, L. Li, F. Lu, C. Lee, A. Burger, J. Trombka, P. Siddons, R.B. James, Proc. SPIE 5198 (2004) 306.
[15] N. Tsoulfanidis, Measurement and Detection of Radiation, second ed., Taylor Francis, Washington, DC, 1995.